

# Inkjet-Printed Quantum Dot–Polymer Composites for Full-Color AC-Driven Displays

By Vanessa Wood, Matthew J. Panzer, Jianglong Chen, Michael S. Bradley, Jonathan E. Halpert, Mounqi G. Bawendi, and Vladimir Bulović\*

We demonstrate print-deposition of high resolution, patterned, multicolored thin films of luminescent colloidal quantum dot (QD)-polymer composites and use the printed patterns in fabricating robust, bright, full-color AC-driven displays. The benefits of AC electroluminescent (EL) displays include simple, low-cost fabrication and high reliability; however, finding efficient and stable phosphors for full-colored displays remains a major challenge.<sup>[1]</sup> Today, red-, green-, and blue-light-emitting (RGB) phosphors for AC-EL comprise different material systems and can have luminous efficiencies that span an order of magnitude, rendering manufacture of a multicolor display with balanced RGB components difficult.<sup>[1–3]</sup> While there has been substantial research on stacked and patterned devices, one of the most feasible strategies for realizing RGB AC-EL displays is color filtering of white, ZnS-based phosphors.<sup>[1,2]</sup> Filtering, however, wastes up to 90% of the output optical power to achieve color saturation, which requires that the display be operated at ten times video brightness in order to meet the RGB color standard.<sup>[4]</sup> This results in greater power consumption, faster pixel degradation, and shorter display lifetimes.<sup>[1]</sup>

To achieve full-color AC-EL displays, in this study we use colloiddally synthesized QDs to print patterns of robust, solution-processable, luminescent light-converting thin films for AC-EL displays. QDs offer narrow-band luminescence that can be tuned across the visible spectrum by varying their size and chemical composition.<sup>[5]</sup> This property motivated the use of QD luminescent centers in thin-film light-emitting diode (LED) structures, in which QDs were electrically excited to demonstrate low-power, color-saturated devices, with side-by-side patterning of RGB pixels enabled by microcontact printing of the QD layers.<sup>[6]</sup> In alternate device designs, QDs can also be optically excited, where, for example, the small Stokes shift of red- and green-light-emitting QDs enables their optical excitation by blue light. This property of QDs led to the demonstration of optical

down-conversion using blue GaN LEDs to excite QDs in poly(laurylmethacrylate) (PLMA), and the generation of point sources of saturated-color light.<sup>[7]</sup> In the present work, we demonstrate a planar, full-color AC-EL display that comprises luminescent thin films of QDs that absorb blue electroluminescence from a commercial phosphor powder and then emit photons at a longer wavelength characteristic of the QD band gap. Emission and absorption spectra for the QDs and EL phosphors

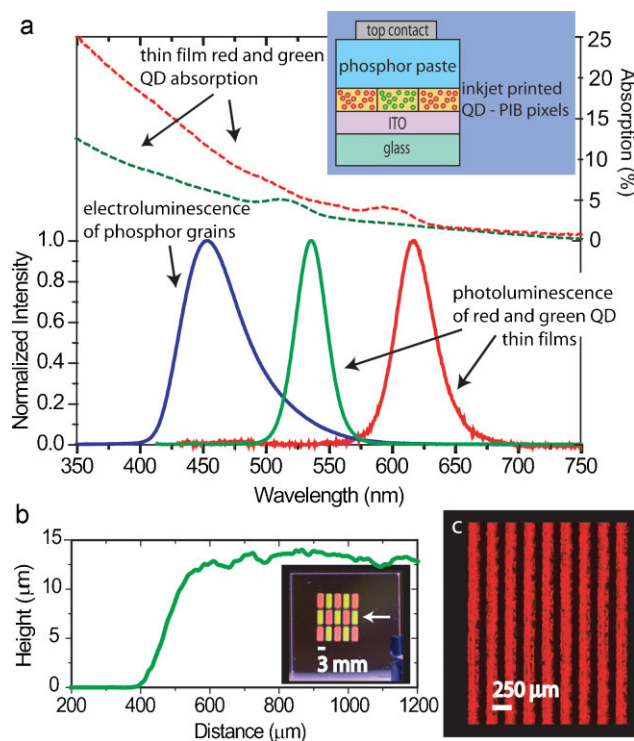


**Figure 1.** a) Absorption and photoluminescence spectra of spin-coated thin films of red and green QDs and the electroluminescence spectrum of the blue-phosphor paste powered by 50 kHz AC excitation demonstrate the spectral overlaps needed to achieve optical down-conversion of phosphor emission to QD-film luminescence. The inset schematic depicts the cross-section of an AC powder EL device structure with QD-PIB pixels. b) 1 mm profilometry scan of the edge of a green rectangular pixel measuring 3 mm × 5 mm demonstrates the edge definition and top-surface uniformity of an average pixel. The inset is a photograph of a multicolor QD-PIB pattern inkjet printed on 1 inch × 1 inch ITO-coated glass and illuminated with  $\lambda = 365$  nm light. c) Luminescence microscopy photograph of a series of parallel lines printed to be 100  $\mu\text{m}$  wide at 250  $\mu\text{m}$  pitch demonstrates the feasibility of printing high-resolution patterns.

[\*] Prof. V. Bulović, V. Wood, Dr. M. J. Panzer, Dr. J. Chen, M. S. Bradley  
Department of Electrical Engineering and Computer Science  
Massachusetts Institute of Technology  
77 Massachusetts Avenue  
Cambridge, MA 02139 (USA)  
E-mail: bulovic@mit.edu

Dr. J. E. Halpert, Prof. M. G. Bawendi  
Department of Chemistry  
Massachusetts Institute of Technology  
77 Massachusetts Avenue  
Cambridge, MA 02139 (USA)

DOI: 10.1002/adma.200803256

used in our work are shown in Figure 1a. In contrast to the earlier work by Taylor et al., which uses a white phosphor and poly[2-methoxy-5-(2'-ethyl-hexyloxy)-1,4-phenylene vinylene] (MEH-PPV) to absorb phosphor luminescence, forming MEH-PPV excitons that are then energy-transferred to QDs,<sup>[8]</sup> our devices operate based entirely on long-range radiative energy transfer, with no short-range Förster energy transfer expected. Consequently, as shown in Figure 1a, we are not limited to red QDs, but can optically excite any QD that has a first absorption peak at a wavelength longer than  $\lambda = 450$  nm.

To deposit thin films of colloiddally synthesized QDs in an AC-EL device, we inkjet-print QD solutions. Inkjet printing is an attractive deposition technique for any large-area electronics application because it minimizes material use and allows for multiple depositions of high-resolution patterned layers of materials. Our experiments show that it is possible to directly inkjet print QDs dispersed in a solvent, but that the structural and luminescent properties of the QD layer are improved if the QDs are embedded in an optically transparent polymer matrix.<sup>[9]</sup> In this paper, we use inkjet printing to deposit well-defined, uniform thin films of QDs suspended in a polyisobutylene (PIB) matrix that exhibit enhanced photoluminescence (PL) efficiency over thin films of QDs. The selection of polyisobutylene (PIB) dissolved in hexane and octane as a base for the QD ink is discussed in the Experimental section and in the Supporting Information. Over a period of several months, we observed no aggregation of QDs in the QD-PIB ink stored in a sealed glass vial, and no degradation or phase separation in printed QD-PIB thin films kept in ambient conditions, indicating a high degree of compatibility between QDs and PIB.

One challenge in inkjet printing a uniform thin film is avoiding the "coffee ring" phenomenon, whereby solutes migrate to the edge of a printed drop during the drying process, forming a thin film of uneven thickness.<sup>[10]</sup> Previous studies have shown that two-solvent techniques can be used to achieve greater uniformity of inkjet printed films and to facilitate deposition of QDs.<sup>[11]</sup> We tune the hexane to octane ratio in the QD-PIB ink solution to reduce nonuniform drying patterns and enable thin films with QDs evenly suspended in a PIB matrix (Supporting Information). A profilometry scan 1 mm long from the indium tin oxide (ITO) to the top surface of a 3 mm  $\times$  5 mm QD-PIB feature (Fig. 1b) demonstrates the edge definition and top-surface uniformity achievable using large droplet sizes and high-speed printing. This feature is comprised of 15 layers of QD-PIB composite printed with 280 pL droplets at a 50  $\mu$ m pitch. Figure 1c, which presents a fluorescence microscopy image of a series of parallel lines printed using 120 pL droplets at a pitch of 250  $\mu$ m, indicates the feasibility of high-resolution patterns. Here, the QD-PIB ratio is tuned to result in lines 100  $\mu$ m wide, where each line is composed of 14 layers of the printed composite to produce printed features 2  $\mu$ m thick. The lack of drift in the printed pattern over the 14 layers and the absence of "coffee ring" features highlight the level of accuracy, uniformity, and repeatability afforded in printing with a QD-polymer composite.

As previous research has shown, embedding QDs in an insulating polymer matrix decreases the amount of QD-luminescence quenching observed in closed-packed QD structures.<sup>[7,12]</sup> We measure, on average, a factor of 2.5 increase in

the PL efficiency for QDs in the PIB matrix as compared to a spin coated, neat thin film of QDs. For both red and green nanoparticles, we inkjet print 10 mm  $\times$  14 mm rectangles of QD-PIB composite and spin-coat solutions of the same nanoparticles on quartz substrates. We measure the PL for each QD-PIB and QD-only sample excited with a  $\lambda = 408$  nm laser, and adjust for the absorption of the sample at  $\lambda = 408$  nm. The PL measurement is performed in 10 different locations across each sample, to account for any nonuniformities across the spin-coated and inkjet printed features. The PL efficiency measurements of the nanoparticle films with and without a PIB binder are described further in the Experimental section.

The basic thin-film AC-EL device structure is shown schematically in the inset of Figure 1a. A detailed description of the device fabrication is provided in the Experimental section, but a brief description is given here. Ink solutions of PIB and QDs in a mixture of hexane and octane are deposited using a Hewlett-Packard thermal inkjet picofluidic dispensing system (TIPS) onto conductive, transparent ITO-coated glass or flexible polyethylene terephthalate (PET). Inkjet printing was demonstrated with a series of PIB-stabilized inks that were formulated for optimized viscosity by mixing PIB with core/shell CdSe/ZnS QDs from QD Vision Inc. and Evident Technologies, as well as with in-house-synthesized QDs and nanorods. The inkjet-printed films of QD-PIB composite were covered with a thin film of ZnS:Cu powder in an electrically insulating, transparent binder from Osram-Sylvania, which is doctor-blade deposited and dried at 50  $^{\circ}$ C. A conductive adhesive tape serves as the top electrode and defines the working device area.

All fabrication and testing was done in ambient conditions and without device packaging. We observed long device shelf lives with no degradation or decrease in brightness during intermittent device testing over one year. The spectra and photographs in Figure 2 show both the blue electroluminescence of the ZnS:Cu phosphors and the green and red QD spectra of optically down-converted QD emission, which is visible when an AC power is applied across the device structures. Because our printing technique results in PIB/QD films of uniform thickness, we were able to demonstrate spectral purity in the optically down-converted QD light with minimal contribution from the blue-phosphor EL emission. When plotted on a Commission International d'Eclairage (CIE) chromaticity diagram (Fig. 2c), the CIE coordinates of our devices define a color triangle that is comparable to the International Telecommunication Union high-definition television (HDTV) standard. Previous work has shown that a solution of mixed QDs can be used to obtain colors inside the space defined by CIE coordinates of the individual QD luminescence.<sup>[11,13]</sup> Now, we demonstrate that by varying the thickness of the printed QD-PIB layer, a single QD-ink solution can be used to achieve the set of colors on the trajectory between the CIE coordinates of the blue phosphor and the CIE coordinates of the particular QD lumophore. For a given printed QD-PIB thickness, we observe little change in the CIE coordinates over the entire range of applied voltages (50–430  $V_{\text{rms}}$ ). While the data in Figure 2 highlights the color uniformity of large (8 mm  $\times$  10 mm) rectangular pixels, it is also possible to fabricate working AC-EL devices with high-resolution features, such as the lines in Figure 1c. Figure 3a is a photoluminescence photograph of a complete device structure on a flexible ITO-coated PET substrate

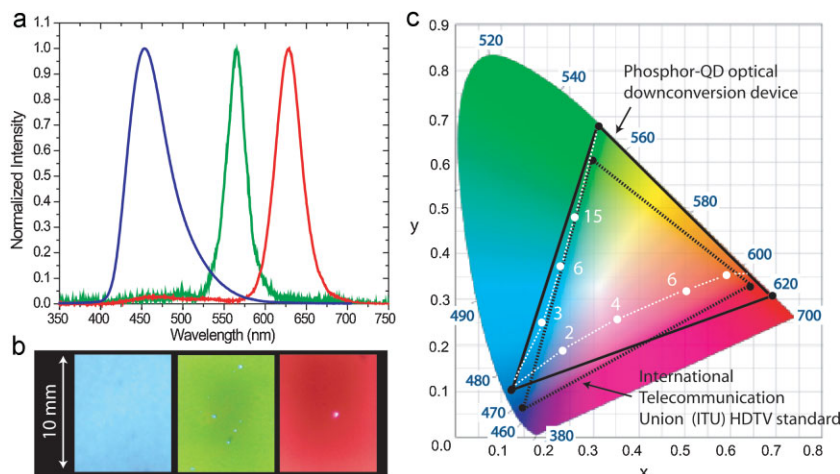


**Figure 2.** a,b) Electroluminescence spectra and photographs of red, green, and blue 80 mm<sup>2</sup> pixels. c) Device CIE coordinates plotted on a chromaticity diagram show that the optical down-conversion devices subtend a color triangle (solid black line) comparable to that of the International Telecommunication Union HDTV standard (dotted black line). The dotted white lines indicate two examples of possible ranges of color that can be obtained by simply varying the thickness of the printed QD-PIB layer fabricated with a single QD-ink solution. The numbers written next to the white data points indicate the number of layers of the QD-PIB ink used to achieve the designated color.

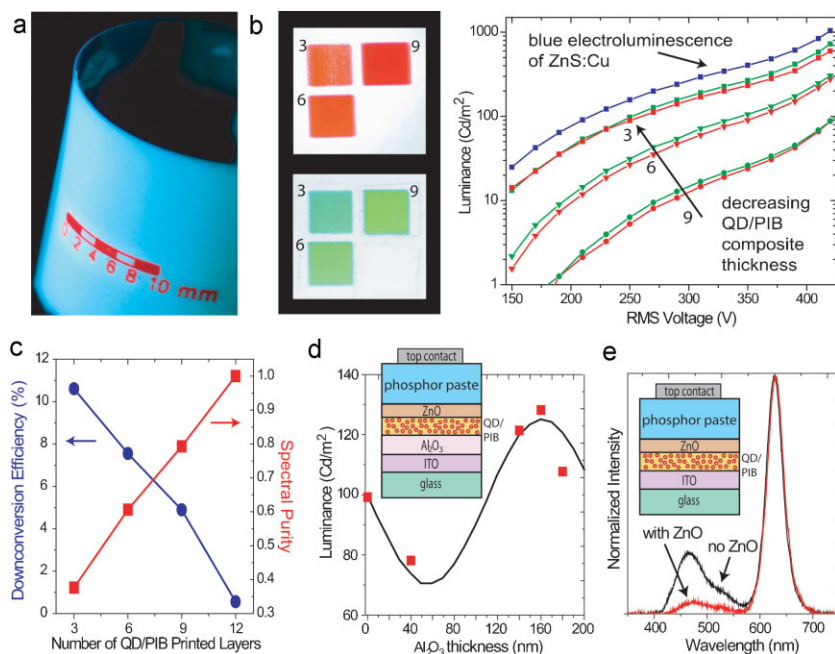


**Figure 3.** a) Photograph of a complete device on a flexible substrate under  $\lambda = 365$  nm wavelength illumination. The ruler pattern printed with red QD-PIB ink is to scale. b) Photographs of the photoluminescence devices with three, six, and nine layers of inkjet-printed QD-PIB under  $\lambda = 365$  nm wavelength illumination, provide a visual indication of the color purity. The plot shows luminance versus applied RMS voltage for a blue (ZnS:Cu phosphor only) pixel as well as the red and green pixels with three, six, and nine layers of QD-PIB. c) Plot of the spectral purity and down-conversion efficiency as a function of QD-PIB-layer thicknesses. d) Data are taken from devices with ZnO layers 50 nm thick and variable thickness of Al<sub>2</sub>O<sub>3</sub> transparent metal oxide layers, positioned as shown with the inset schematic. The plot shows measured (data points) and modeled (black line) device luminance as a function of Al<sub>2</sub>O<sub>3</sub> layer thickness. The data follow the oscillatory trend predicted by the model described in the text. e) The electroluminescence spectra for devices with and without a 20 nm ZnO layer indicate that the ZnO contributes to wave-guiding of the phosphor electroluminescence in the plane of the substrate, which facilitates an improved color purity of the emission. The inset schematic shows the placement of the ZnO layer in the device structure.

with a ruler pattern that marks off 2 mm divisions for a 1 cm shape printed to scale.

We measure luminance as a function of applied AC voltage for devices with different numbers of printed red and green QD-PIB layers, as well as for blue (ZnS:Cu phosphor only) devices (Fig. 3b). The luminance versus RMS-voltage plot highlights the tradeoff between spectral purity and brightness at a specific driving voltage. As shown in Figure 3c, the spectral purity, defined as the fraction of the device electroluminescence spectrum comprised of QD emission, increases as a function of the number of QD-PIB layers. The down-conversion efficiency, which we define as the ratio of the watts of QD emission collected to the watts of the phosphor emission created, decreases as a function of the number of QD-PIB layers. These trends provide insight into the performance of our devices. For a thin QD-PIB layer (2  $\mu$ m thick), we measure down-conversion efficiencies near 12%. This is consistent with the 15% PL efficiency of the QDs in the PIB matrix with additional losses due to QD light self-absorption. As the thickness of the QD-PIB layer increases, less blue light reaches the QDs furthest from the phosphor layer, while lower-energy emission from the layer of QDs closest to the phosphor is subject to more scattering and reabsorption.

The luminous efficiency of our devices is approximately 0.1 lm W<sup>-1</sup> for the blue phosphor driven with 420 V<sub>rms</sub> at 31 kHz, which is comparable to commercially available AC-power EL devices.<sup>[1]</sup> The electronic properties of the device are dominated by the thick phosphor layer (500  $\mu$ m in thickness), so small changes in the QD-PIB layer thickness do not contribute substantially to variation in the input power needed to drive the device.

Device luminance can be increased when additional transparent metal oxide layers are inserted into the device structure. We limit our choice of metal oxides to materials that are robust insulators, and investigate device structures with metal oxides on either side of the QD-PIB composite layer, such as the one shown schematically in the inset of Figure 3d. To determine the layer thicknesses of the metal oxides needed to simultaneously maximize absorption of the phosphor luminescence by the QDs and the transmission of the QD luminescence through the glass to the viewer, we model the device as a dielectric stack.<sup>[14]</sup> We use a transmission and propagation numerical-simulation matrix method and integrate over all emission angles to account for off-normal transmission and reflection, as

well as wave-guided luminescence. The simulation also accounts for the wavelength dependence of the absorption and emission profiles of the different layers. We apply the Maxwell–Garnett mixing rule relation to determine values of the index of refraction for the phosphor ( $n = 2.3$ ) and the QD–PIB layer ( $n = 1.8$ ).<sup>[1,15]</sup> The complex part of the QD index of refraction is calculated from the absorption data of QD–PIB films printed on glass substrates. We find that ZnO, which has an index of approximately 2.0 in the visible-light wavelength range, is a desirable buffer layer between the phosphor and the QD–PIB matrix, as it laterally waveguides some of the phosphor electroluminescence, which facilitates an improved color purity of the top-surface QD emission. To minimize wave-guiding of the QD emission in the ITO layer (refractive index  $\approx 2.0$ ), the lower index  $\text{Al}_2\text{O}_3$  ( $\approx 1.6$ ) can be inserted between the ITO and the QD–PIB layer. Our model indicates that transmission of QD luminescence to the viewer is maximized using a layer of ZnO 50 nm thick and a layer of  $\text{Al}_2\text{O}_3$  160 nm thick.

To demonstrate that predicted trends in luminance are indeed observed, we fabricate devices with layers of ZnO and/or  $\text{Al}_2\text{O}_3$ . We deposit the metal oxides with radio frequency magnetron sputtering, which has been shown to be compatible with QDs in a LED structure and is a common, low-cost, and low-temperature technique for depositing thin-film coatings.<sup>[6c]</sup> We fabricate devices, as shown in Figure 3d, with  $\text{Al}_2\text{O}_3$ -film thicknesses of 0, 40, 140, 160, and 180 nm on ITO, followed by nine inkjet-printed QD–PIB layers, and 50 nm of ZnO. Figure 3d plots luminance measured at 420 V<sub>rms</sub> and 31 kHz versus  $\text{Al}_2\text{O}_3$  thickness for these devices. The data follow the oscillatory trend predicted by the optical modeling. To demonstrate the wave-guiding effect in the ZnO layer, we fabricate devices with and without a 20 nm layer of ZnO on top of the QD–PIB composite. As shown by the device electroluminescence spectra in Figure 3e, the ZnO layer wave-guides the phosphor emission in the plane of the substrate, decreasing the transmission of blue light to the viewer while still allowing excitation of the QDs. The demonstrated use of sputtered metal oxide films in the device structures confirms that the inkjet-printing technique is compatible with AC thin-film EL devices in which two thick insulating layers, such as  $\text{Al}_2\text{O}_3$ , surround a crystalline phosphor layer.<sup>[1]</sup>

In conclusion, we have demonstrated a simple and scalable method to achieve patterned pixels for flexible, full-color, large-area, AC-driven displays operating at video brightness. We have shown that a QD–polymer composite can be printed using stable ink solutions, and that it contributes to an efficient and robust device architecture. Optimization of the QD–polymer composite layer thickness can be used to tune luminance and color for specific applications. Finally, our inkjet-printing technique is well-suited for integration with metal oxide dielectric layers, which can enable improved optical and electrical performance.

## Experimental

The QD–PIB ink solution is a mixture of PIB and colloidal QDs dispersed in hexane and octane. 400 000 molecular-weight PIB (Acros #17818) was dissolved in hexane and octane (0.1 g PIB per 10 mL hexane and 1 mL of octane). The appropriate ratio of hexane to octane was

determined experimentally, as described in the Supporting Information. This PIB solution was then mixed with a solution with 2 mg mL<sup>-1</sup> concentration of QDs in hexane in proportions of one part PIB solution to between two and four parts QD solution. The exact optimal proportion for inkjet printing was based on desired drop size and QD-loading fraction. Successful prints were demonstrated with inks that used nanoparticles from a variety of sources. CdSe/ZnS QDs were obtained from QD Vision Inc. and from Evident Technologies Inc., with solution photoluminescences of the various QDs peaked at wavelengths of 530 nm, 547 nm, 612 nm, and 614 nm. To remove excess ligands, the QDs were repeatedly crashed out in methanol and then redispersed in hexane. In-house-synthesized CdSe/ZnS QDs and nanorods with solution photoluminescences peaked at wavelengths of 608 and 630 nm were also used.

Devices were fabricated with a layer-by-layer approach that was compatible with flexible substrates. The QD–PIB inks were printed on conductive ITO. The ITO was obtained on glass substrates from Thin Films Inc. or on flexible polyethylene terephthalate (PET) substrates from Sheldahl Inc. Printing was realized with a Hewlett–Packard Thermal Inkjet Picofluidic dispensing System (TIPS) operated in conjunction with a Labview controlled precision movable stage. Patterns in this work were formed with 50–300 pL drop volumes, deposited at a 50  $\mu\text{m}$  to 100  $\mu\text{m}$  pitch.

The blue phosphor used in this study was Type 813 ZnS:Cu powder dispersed in electroluminescent binder from Osram-Sylvania. This phosphor was doctor-blade-deposited with a 500  $\mu\text{m}$  thickness using a disposable mask to define the active device area and the bottom ITO contacts. The sample was dried at 50 °C for 2 h. Top contacts were produced using conductive tape from 3M (# 9713). This basic device structure was assembled and tested entirely in ambient conditions.

$\text{Al}_2\text{O}_3$  and ZnO metal oxide layers were deposited using radio-frequency magnetron sputtering in an inert Ar environment at 4 mTorr (1 Torr = 133.32 Pa). The metal oxide layers were deposited using sputtering targets with 3 inch diameter mounted on US Inc. sputtering guns with a power of 150 W used for the  $\text{Al}_2\text{O}_3$  deposition and 25 W for the ZnO deposition, corresponding to deposition rates of 0.4  $\text{\AA s}^{-1}$  and 0.2  $\text{\AA s}^{-1}$ , respectively.

Photographs of PL were taken with the sample illuminated with a UV lamp at a wavelength of 365 nm. PL spectral measurements were obtained with the sample excited using a 408 nm wavelength laser. The electroluminescence and PL spectra were taken with an Acton Research SpectraPro 300i. Absorption was determined from reflection and transmission measurements taken using a Cary 500i spectrophotometer. The diffuse reflectance accessory was used to measure the absorption of the QD–PIB matrix. PL efficiencies of the spun-cast QD thin films and the inkjet-printed QD–PIB layers were determined by comparing the number of photons emitted from the samples and the sample absorption at  $\lambda = 408$  nm against the same measurements on a tris-(8-hydroxyquinoline) aluminum ( $\text{Alq}_3$ ) standard.

Voltage-dependent measurements were performed with a 31 kHz AC signal provided by a JKL inverter (BXA-24529). Lower-voltage, frequency-dependent measurements were taken using a Hewlett–Packard 3245A Universal Source. Luminance measurements and CIE coordinates were obtained using a Konica–Minolta CS-200 luminance and color meter. Input power to the device was calculated measuring the voltage drops across the device and a series resistor and the phase angle between the two signals using a Tectronix TDS 3054B oscilloscope.

## Acknowledgements

The authors thank QD Vision Inc. for supplying quantum dots used in this work and Sheldahl Inc. for providing flexible ITO-coated PET substrates. We also thank Dr. M. Chaparala (Hewlett Packard), G. Su, and P. Anikeeva for their assistance and helpful discussions. This work made use of MRSEC Shared Experimental Facilities at MIT, supported by the National Science Foundation under award number DMR-02-13282. Funding for this project was provided by the Institute for Soldier Nanotechnologies, the DARPA

MIT-OSU-HP Focus Center on Non-Lithographic Technologies for MEMS/NEMS, a Presidential Early Career Award for Scientists and Engineers, and a NDSEG Fellowship. Supporting Information is available online from Wiley InterScience or from the author.

Received: November 5, 2008

Revised: December 23, 2008

Published online: March 4, 2009

- 
- [1] Y. A. Ono, *Electroluminescent Displays*, World Scientific, Singapore **1995**.  
 [2] C. N. King, *J. Vac. Sci. Technol. A* **1996**, *14*, 1729.  
 [3] a) T. Minami, *Solid-State Electron.* **2003**, *47*, 2237. b) K. Tanaka, Y. Kimura, S. Okamoto, Y. Inoue, K. Sato, *Jpn. J. Appl. Phys. Part 1* **1998**, *37*, 3350.  
 [4] P. E. Burrows, G. Gu, V. Bulović, Z. Shen, S. R. Forrest, M. E. Thompson, *IEEE Trans. Electron Devices* **1997**, *44*, 1188.  
 [5] C. B. Murray, D. J. Norris, M. G. Bawendi, *J. Am. Chem. Soc.* **1993**, *115*, 8706.  
 [6] a) S. Coe, W.-K. Woo, M. G. Bawendi, V. Bulović, *Nature* **2002**, *420*, 800. b) J. S. Steckel, J. P. Zimmer, S. Coe-Sullivan, N. E. Stott, V. Bulović, M. G. Bawendi, *Angew. Chem. Int. Ed.* **2004**, *43*, 2154. c) S. Coe-Sullivan, J. S. Steckel, L. A. Kim, M. G. Bawendi, V. Bulović, *Light-emitting Diodes: Research, manufacturing, and Applications IX*, Proc. SPIE (Eds: S. A. Stockman, H. W. Yao, E. F. Schubert), San Jose **2005**, pp. 108-115. d) J. S. Steckel, P. Snee, S. Coe-Sullivan, J. P. Zimmer, J. E. Halpert, P. Anikeeva, L. A. Kim, V. Bulović, M. G. Bawendi, *Angew. Chem. Int. Ed.* **2006**, *45*, 5796. e) J. M. Caruge, J. E. Halpert, V. Wood, V. Bulović, M. G. Bawendi, *Nat. Photonics* **2008**, *2*, 247.  
 [7] J. Lee, V. C. Sundar, J. R. Heine, M. G. Bawendi, K. F. Jensen, *Adv. Mater.* **2000**, *12*, 1102.  
 [8] R. M. Taylor, K. H. Church, M. I. Sluch, *Displays* **2007**, *28*, 92.  
 [9] M. Böberl, M. V. Kovalenko, S. Gamerith, E. J. W. List, W. Heiss, *Adv. Mater.* **2007**, *19*, 3574.  
 [10] a) R. D. Deegan, O. Bakajin, T. F. Dupont, G. Huber, S. R. Nagel, T. A. Witten, *Nature* **1997**, *389*, 827. b) R. D. Deegan, O. Bakajin, T. F. Dupont, G. Huber, S. R. Nagel, T. A. Witten, *Phys. Rev. E* **2000**, *62*, 756.  
 [11] a) S. Coe-Sullivan, J. S. Steckel, W. K. Woo, M. G. Bawendi, V. Bulović, *Adv. Funct. Mater.* **2005**, *15*, 1117. b) E. Tekin, P. J. Smith, S. Hoepfner, A. M. J. van de Berg, A. S. Susha, A. L. Rogach, J. Feldmann, U. S. Schubert, *Adv. Funct. Mater.* **2007**, *17*, 23. c) J. A. Lim, W. H. Lee, H. S. Lee, J. H. Lee, Y. D. Park, K. Cho, *Adv. Funct. Mater.* **2008**, *18*, 229.  
 [12] D. E. Fogg, L. H. Radzilowski, R. Blanski, R. R. Schrock, E. L. Thomas, M. G. Bawendi, *Macromolecules* **1997**, *30*, 417.  
 [13] P. O. Anikeeva, J. E. Halpert, M. G. Bawendi, V. Bulović, *Nano Lett.* **2007**, *7*, 2196.  
 [14] J. A. Kong, *Electromagnetic Wave Theory*, EMW Publishing, Cambridge **2000**.  
 [15] A. Sihvola, *Subsurf. Sens. Technol. Appl.* **2000**, *1*, 393.
-